Exact quantum, quasiclassical, and semiclassical reaction probabilities for the collinear $F+H_2 \rightarrow FH+H$ reaction*

George C. Schatz,† Joel M. Bowman,‡ and Aron Kuppermann

Arthur Amos Noyes Laboratory of Chemical Physics,§ *California Institute of Technology, Pasadena, California 91125*
(Received 22 October 1974)

Exact quantum, quasiclassical, and semiclassical reaction probabilities and rate constants for the collinear reaction $F+H_2 \rightarrow FH+H$ are presented and compared. The exact quantum results indicate a large degree of population inversion of the FH product with P_{02}^R and P_{03}^R being the dominant reaction probabilities. The energy dependence of these two probabilities at low translational energies are quite different. P_{02}^R shows an effective threshold of 0.005 eV which can largely be interpreted as resulting from tunneling through a vibrationally adiabatic barrier. P_{03}^R has a much larger effective threshold (0.045 eV) apparently resulting from dynamical effects. Quasiclassical probabilities for the collinear $F+H_2$ reaction were calculated by both the forward (initial conditions chosen for reagent $F+H_2$) and reverse (initial conditions for product H+FH) trajectory methods. The results of both calculations correctly indicate that P_{03}^R and P_{02}^R should be the dominant reaction probabilities. However, the threshold behavior of the quasiclassical forward P_{03}^R disagrees strongly with the corresponding exact quantum threshold energy dependence. By contrast, there is good agreement between the reversed trajectory results and the exact quantum ones. The uniform semiclassical results also agree well with the corresponding exact quantum ones indicating that the quasiclassical reverse and the semiclassical methods are preferable to the quasiclassical forward method for this reaction. The important differences between the threshold behavior of the exact quantum and quasiclassical forward reaction probabilities are manifested in the corresponding rate constants primarily as large differences in their activation energies. Additional exact quantum results at higher total energies indicate that threshold effects are no longer important for reactions with vibrationally excited H_2. Resonances play an important role in certain reaction probabilities primarily at higher relative translational energies.

I. INTRODUCTION

The reactions $F+H_2(D_2, DH) \rightarrow FH\ (FD) + H\ (D)$ have recently been the subject of several experimental studies in which very detailed rate constants and cross sections for these reactions have been measured. Relative rate constants into specific vibrational (and sometimes vibrational–rotational) states of the products have been measured by both infrared chemiluminescence[1] and chemical laser[2] techniques and, quite recently, both methods have been used to study the temperature dependences of these relative rates.[1f,2d] Angular distributions for specific product vibrational states of the $F+D_2$ reaction have been studied at several incident energies by a crossed molecular beam apparatus.[3] In addition, there exist several (usually indirect) determinations of the over-all bulk rate constants for the $F+H_2$ reaction[4] and, more recently, studies of isotope effects for the $F+H_2$, $F+D_2$, $F+HD$, and $F+DH$ series.[5] A very important application of these reactions has been to the fluorine–hydrogen chemical lasers,[2a,6] where $F+H_2 \rightarrow FH+H$ serves as the main pumping reaction.

Complementing these experimental studies have been several quasiclassical trajectory studies on $F+H_2$[7,8,9], $F+D_2$[7,10,11] and $F+DH(HD)$,[7,9] and one recent semiclassical study on collinear $F+D_2$.[12] The results of the quasiclassical studies have generally been in reasonably good agreement with the detailed rate constants obtained by infrared chemiluminescence and chemical laser experiments but in much poorer agreement with the angular distributions obtained by the molecular beam experiments. There also exists some disagreement between experiment and the classical calculations on the rotational distribution of the detailed rate constants,[7b] and on isotope effects.[5] Additional theoretical developments have been the characterization of the product state distributions by temperaturelike parameters,[13] and the establishment of a relationship between these parameters and certain details of the potential energy surface.[14] All of the classical theoretical studies have employed semiempirical potential energy surfaces.[7–11] An *ab initio* potential energy surface has also been calculated,[15] and the semiempirical surfaces are in reasonable agreement with it.

Aside from possible defects in the potential energy surface used, the most important sources of disagreement between the quasiclassical trajectory calculations and experiment are (a) electronically nonadiabatic effects, and (b) quantum dynamical effects. The first problem has been discussed by various investigators,[16–18] but its importance is not completely understood at present and we shall not consider it here.

In this paper, we study the importance of quantum dynamical effects in the $F+H_2 \rightarrow FH+H$ reaction by comparing the results of accurate quantum mechanical solutions to the Schrödinger equation for the collinear collisions to the results of the corresponding quasiclassical and semiclassical calculations. In the following paper (hereafter referred to as II), we make the analogous study for the $F+D_2$ reaction and also examine exact quantum results for $F+HD(DH)$. Results of our preliminary studies[19,20] indicated that quantum effects were quite important in the collinear $F+H_2$ reaction[19] and, in fact, the disagreement between the quasiclassical and exact quantum reaction probabilities at low reagent relative translational energies was quite large. In the present paper, we give a more detailed analysis of the reaction probabilities for $F+H_2$ as calculated by four different methods: an exact quantum mechanical solution, the quasiclassical forward and quasiclassical re-

Copyright © 1975 American Institute of Physics

Downloaded 21 Dec 2005 to 131.215.225.171. Redistribution subject to AIP license or copyright, see http://jcp.aip.org/jcp/copyright.jsp

verse trajectory methods, and the uniform semiclassical method. We also present and compare the corresponding rate constants obtained from the results of these four methods. In addition, we examine resonances, tunneling, and energy partitioning in this reaction, and examine the results of exact quantum calculations at total energies for which two vibrational states of the reagent H_2 are accessible.

In all cases, we restrict our considerations to collinear collisions of a fluorine atom with a hydrogen molecule where the two hydrogen atoms are considered to be distinguishable. The resulting cross sections are in the form of dimensionless probabilities of reaction between specific vibrational states of the reagents to form products in specific states and are not directly comparable with experiment (although certain other quantities such as final state distributions can, with caution, be subject to such a comparison). Our justification for studying collinear dynamics lies mainly in its use as a predictive model for the energy release behavior in actual three-dimensional collisions[21] and as a testing ground for approximate theories of chemical dynamics.[22] Exact quantum dynamics is currently feasible for many types of collinear reactions, and thus the importance of quantum effects in chemical reactions can readily be established within the collinear restriction. How these quantum effects will be modified in two- or three-dimensional systems has not yet been fully established, but some progress has been made towards obtaining exact quantum solutions to these problems,[23] and quite recently accurate converged results have been obtained for the $H + H_2$ coplanar and 3-D exchange reaction.[24]

In Sec. II, the potential energy surface used in our calculations is described. In Sec. III we compare the quantum, quasiclassical, and semiclassical reaction probabilities for $F + H_2$, and in Sec. IV we compare the corresponding rate constants. Reaction probabilities for $F + H_2$ in the higher total energy range where two reagent vibrational states are open are discussed in Sec. V, and in Sec. VI is a short summary.

II. POTENTIAL ENERGY SURFACE

We used the semiempirical LEPS potential energy surface of Muckerman[12,25] (his surface 5). This surface is intermediate in character between his surfaces 2 and 3 of Ref. 7b and was chosen to optimize agreement between his three-dimensional trajectory results and experiment.[7b,12] Using Muckerman's notation, the parameters describing the extended LEPS surface are D_e (HF) $= 6.1229$ eV, $\beta_e(\mathrm{HF}) = 2.2187$ Å^{-1}, $R_e(\mathrm{HF}) = 0.9170$ Å, $\Delta(\mathrm{HF}) = 0.167$, $D_e(\mathrm{H_2}) = 4.7462$ eV, $\beta_e(\mathrm{H_2}) = 1.9420$ Å^{-1}, $R_e(\mathrm{H_2}) = 0.7149$ Å, and $\Delta(\mathrm{H_2}) = 0.106$. The exothermicity is 1.3767 eV (31.76 kcal/mole) and the barrier height 0.0461 eV (1.06 kcal/mole). Figure 1 shows an equipotential contour plot of the collinear surface along with the minimum energy path. The coordinate system for the plot (and for all calculations) is chosen to diagonalize the kinetic energy with a single reduced mass and is defined by[26]

$$x_1' = \left(\frac{\mu_{F,HH}}{\mu_{HH}}\right)^{1/4} \left(r_{HF} + \frac{\mu_{HH}}{m_H} r_{HH}\right),$$

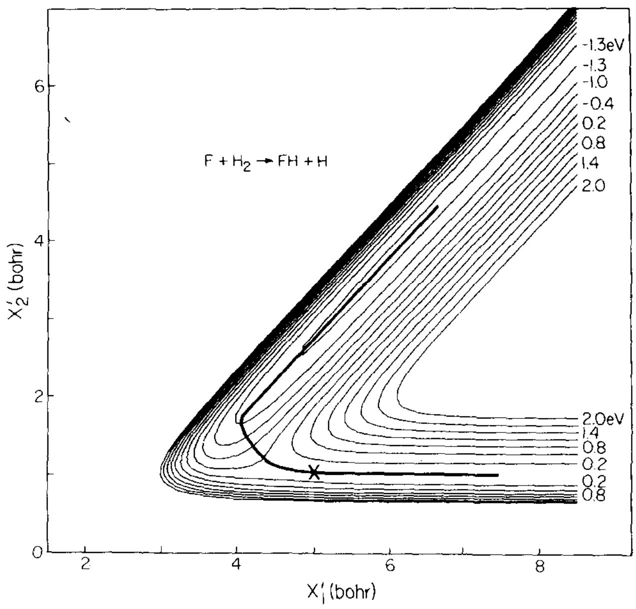

FIG. 1. Equipotential contour plot of the FH_2 collinear potential energy surface used in all calculations reported here. Energies given are relative to the minimum in the H_2 diatomic potential curve. Coordinate system is defined in text. Heavy line denotes the minimum energy path with saddle point indicated by a cross.

$$x_2' = \left(\frac{\mu_{HH}}{\mu_{F,HH}}\right)^{1/4} (r_{HH}),$$

where r_{HF} is the shorter of the two HF bond distances in the H–H–F linear geometry. The analogous coordinate system appropriate for the product arrangement channel (FH + H) is

$$z_1' = \left(\frac{\mu_{H,FH}}{\mu_{FH}}\right)^{1/4} \left(r_{HH} + \frac{\mu_{FH}}{m_H} r_{HF}\right),$$

$$z_2' = \left(\frac{\mu_{HF}}{\mu_{H,FH}}\right)^{1/4} (r_{HF}).$$

These coordinate systems have the advantage over others[27] in that the transformation between the (x_1', x_2') coordinate system appropriate for reagents and the (z_1', z_2') system appropriate for the products is orthogonal.

Since the vibrational spacing in H_2 is about 12 kcal/mole and that in HF is 11 kcal/mole, four vibrational states of HF are normally accessible for thermal distributions of reagent H_2 due to the exothermicity of the reaction.

III. QUANTUM, QUASICLASSICAL, AND SEMICLASSICAL REACTION PROBABILITIES FOR COLLINEAR $F + H_2 \rightarrow FH + H$

A. Exact quantum reaction probabilities

1. Numerical method

We used the close coupling propagation method of Kuppermann[28] to solve the Schrödinger equation for the collinear system $F + H_2$. The method involves dividing the configuration space depicted in Fig. 1 into different regions and then propagating though a given region in a

Downloaded 21 Dec 2005 to 131.215.225.171. Redistribution subject to AIP license or copyright, see http://jcp.aip.org/jcp/copyright.jsp

coordinate system appropriate to that region. In particular, rectangular coordinates were used in the near asymptotic regions appropriate to reagents and products and polar coordinates in the strong interaction region with the origin of the coordinate system chosen in the classically inaccessible plateau area corresponding to dissociation. A basis set of pseudovibrational eigenfunctions describing motion transverse to the direction of propagation was used for expanding the wavefunctions. These eigenfunctions were calculated by a finite difference procedure,[29] and the basis set was changed often during the propagation to insure an efficient representation of the wavefunction. Contributions from continuum vibrational channels are not included in this method. The integration of the coupled Schrödinger equation was done with an Adams–Moulton 4th order predictor—4th order corrector method (with a 4th order Runge–Kutta–Gill initiator). The procedure for extracting the probability matrices from the asymptotic solutions is similar to that used by Truhlar and Kuppermann.[22] Convergence of the final reaction probabilities was carefully checked by observing the effect of varying the location of the origin of the polar coordinate system, location of the end point of the integration,[30] number of closed vibrational channels, number of integration steps, and number of grid points in the finite difference eigenfunction determination. Using 12 to 15 vibrational channels throughout the integration, we obtained a scattering matrix for

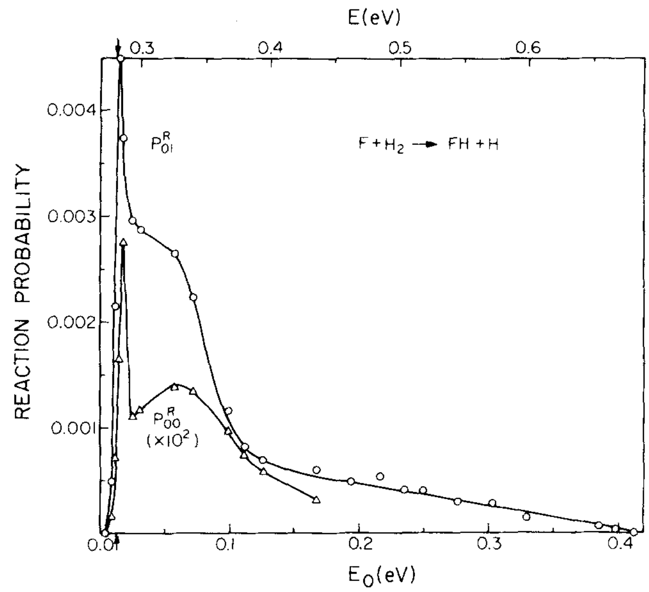

FIG. 3. Exact quantum reaction probabilities P^R_{01} and P^R_{00} (similar to Fig. 2).

which unitarity and symmetry were deemed adequate (flux conservation to 0.5% and symmetry to 5% or better) in the reagent translational energy range (relative to $\nu = 0$) $E_0 = 0.0$ to 1.10 eV. The computation time for a 13 channel calculation on an IBM 370-158 computer was approximately 32 min for the initial calculation in which a large amount of energy independent information was stored on disk for subsequent use and 5 min per energy thereafter.

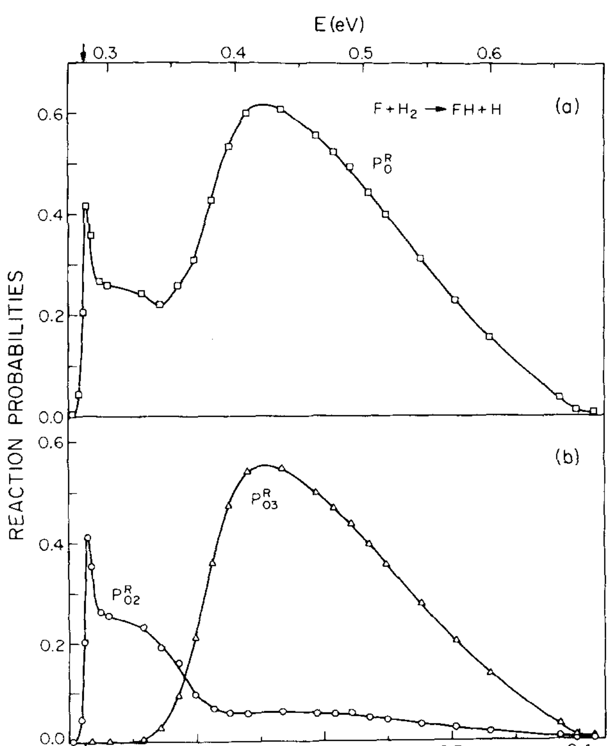

FIG. 2. Exact quantum reaction probabilities for collinear $F + H_2$ as a function of relative translational energy E_0 and total energy E (relative to minimum in H_2 diatomic potential energy curve). (a) Total reaction probability P^R_0 from $\nu = 0$ of H_2; (b) reaction probabilities P^R_{02} and P^R_{03} (defined in text). Vertical arrow in abscissa indicates the energy at which $\nu = 3$ of HF becomes accessible.

2. *Results*

We define the probability of reaction from an initial state ν (of the reagent H_2) to a final state ν' (of the product HF) by the symbol $P^R_{\nu\nu'}$. (This symbol will also be used as a shorthand notation for the phase "$\nu \rightarrow \nu'$ reactive collision.") The total reaction probability P^R_ν from a given incident state ν is the sum of $P^R_{\nu\nu'}$ over all accessible ν'. The exact quantum (EQ) reaction probabilities P^R_{02}, P^R_{03}, and P^R_0 for $F + H_2$ in the translational energy range $E_0 = 0.0$–0.4 eV are presented in Fig. 2. The reaction probabilities for the transitions P^R_{00} and P^R_{01}, which are also allowed in this E_0 range, are plotted in Fig. 3. We see that P^R_{00} and P^R_{01} have an energy dependence very similar to P^R_{02}, but with much smaller values ($P^R_{00} \simeq 6 \times 10^{-5}\, P^R_{02}$, $P^R_{01} \simeq 1 \times 10^{-2}\, P^R_{02}$). As a result, only P^R_{02} and P^R_{03} contribute appreciably to P^R_0 in the energy range considered. As was pointed out previously,[19] P^R_{02} and P^R_{03} have remarkably different threshold behaviors. We shall define the effective threshold energy E_T for the $\nu \rightarrow \nu'$ transition as the difference between the (lowest) energy for which the corresponding $P^R_{\nu\nu'}$ is equal to, say, 1% of the maximum value attained by this quantity and the energy at which the $\nu \rightarrow \nu'$ process becomes energetically possible. With this definition, P^R_{02} has an effective threshold of 0.005 eV, while for P^R_{03} (which is energetically forbidden until $E_0 = 0.013$ eV), E_T is 0.045. Note that while the barrier height is 0.0461 eV, the zero point energy of H_2 is 0.268 eV, so the transition P^R_{02} is energetically allowed even at

Downloaded 21 Dec 2005 to 131.215.225.171. Redistribution subject to AIP license or copyright, see http://jcp.aip.org/jcp/copyright.jsp

zero translational energy. Likewise the $0 \rightarrow 3$ reactive transition is energetically allowed as the HF(3) channel opens up at $E_0 = 0.013$ eV. One possible explanation for why the effective threshold of P_{02}^R is greater than zero is that the exchange of energy between motion transverse to the reaction coordinate and that along the reaction coordinate is not efficient (at least in the entrance channel region of configuration space where the saddle point lies). Truhlar and Kuppermann have shown[22] that a more realistic estimate of the effective barrier height in $H + H_2$ is obtained from vibrationally adiabatic theory. The vibrationally adiabatic barrier (for zero curvature and using the harmonic approximation) for $F + H_2$ is 0.026 eV, which is still appreciably larger than the effective quantum threshold energy for P_{02}^R (0.005 eV), although it is quite close to the P_{02}^R quasiclassical threshold energy (0.025 eV) (see Sec. III. B. 2). This difference between the quantum and quasiclassical threshold energies could in part be due to tunneling through the one-dimensional adiabatic barrier, within the framework of an adiabatic description of the quantum dynamics in the neighborhood of the saddle point. In Paper II we shall see that the results for $F + D_2$, $F + HD$, and $F + DH$ support this conclusion. The high threshold energy for P_{03}^R is not easily explained as resulting from one-dimensional adiabatic barrier tunneling and is probably due to a dynamical effect, as will be discussed in Sec. III. B. 2.

The sharp spike in the P_{02}^R curve at energies slightly above threshold is reminiscent of the Feshbach type internal excitation resonances observed in the collinear $H + H_2$ reaction.[31] A discussion of other resonances in the $F + H_2$ reaction is presented in Sec. V.

Simultaneously with the reactive transition probabilities, we have calculated the nonreactive ones corresponding to the collisions $F + H_2(0) \rightarrow F + H_2(0)$ and $FH(\nu) + H \rightarrow FH(\nu') + H$. The probabilities for the first of these nonreactive processes are simply the difference between unity and the total reaction probability P_0^R (as long as $\nu = 1$ of H_2 is closed). The transition probabilities for the $H + HF(\nu')$ inelastic ($\nu' \neq \nu$) processes are all quite small (generally less than 0.01) up to $E_0 = 0.4$ eV and vary relatively slowly with energy. Unitarity of the scattering matrix then forces the elastic probabilities for $H + HF(\nu)$ collisions to be roughly equal to the difference between unity and the probability for the $F + H_2(0) \rightarrow FH(\nu) + H$ reactive process. The behavior of the inelastic transition probabilities for nonreactive $H + HF$ collisions contrasts strongly with the corresponding inelastic transition probabilities for collinear $H + FH$ collisions.[32] In the latter case we find that the probability of an inelastic collision is comparable in magnitude to the elastic transition probabilities and, in addition, the probabilities of multiquantum jump transitions are often greater than the probabilities of single quantum jump transitions. A more complete discussion of the results for collinear $H + FH$ will be given in Ref. 32.

B. Quasiclassical reaction probabilities

1. Method

The classical trajectory calculations were carried out in the same way as in a previous $H + H_2$ study.[33,34] The initial phase angle variable for the vibration of the ground state of H_2 was varied uniformly over a grid of typically 100 points in the interval 0 to 2π. The final action number of the product HF was computed for each reactive trajectory and assigned a quantum number by rounding off the action number to the nearest integer. Thus, the transition probability $P_{0\nu'}^R$ was defined as the fraction of reactive trajectories with final quantum number ν'.

When this procedure is carried out in the direction $F + H_2(\nu = 0) \rightarrow FH(\nu') + H$, we term the quasiclassical transition probabilities "quasiclassical forward" (QCF). For the reverse reaction, the quasiclassical transition probabilities are termed "quasiclassical reverse" (QCR). Quantum mechanically, the forward and reverse probabilities are rigorously equal at the same total energy, but quasiclassically they are not.[20] Therefore, either of the two quasiclassical results, QCF or QCR, could be used to represent the probabilities for the (forward) reactive collisions. Since there is presently no *a priori* way of deciding which of these two procedures will give results closer to the EQ ones, we have used them both, and corresponding results are presented below.

2. Results

In Fig. 4 we plot the QCF and EQ reaction probabilities P_{02}^R, P_{03}^R, and P_0^R vs the translational energy E_0, as

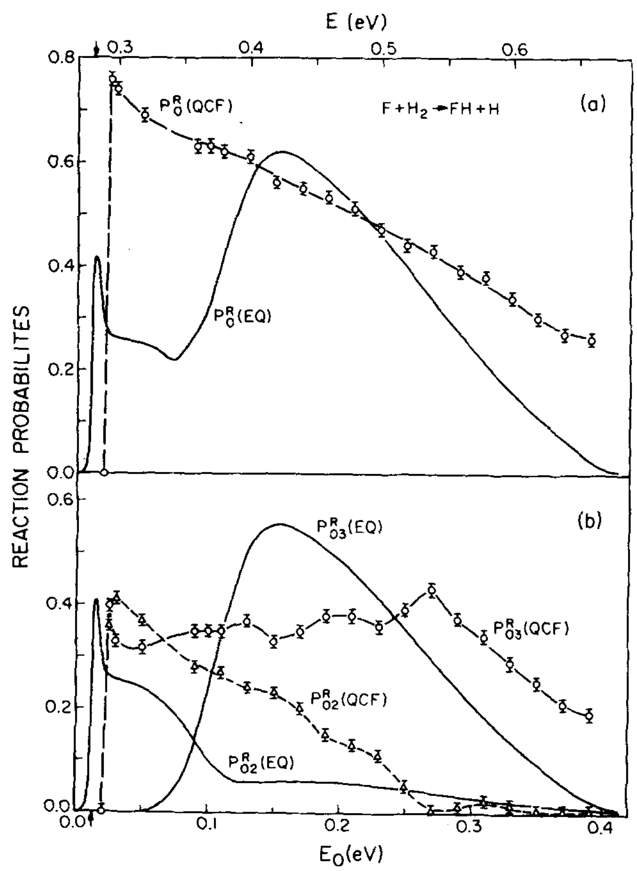

FIG. 4. Quasiclassical forward and exact quantum reaction probabilities for $F + H_2$: (a) P_0^R, (b) P_{02}^R and P_{03}^R. Dashed line indicates QCF results with their associated statistical errors indicated by vertical bars. Solid line indicates EQ results (as in Fig. 2).

Downloaded 21 Dec 2005 to 131.215.225.171. Redistribution subject to AIP license or copyright, see http://jcp.aip.org/jcp/copyright.jsp

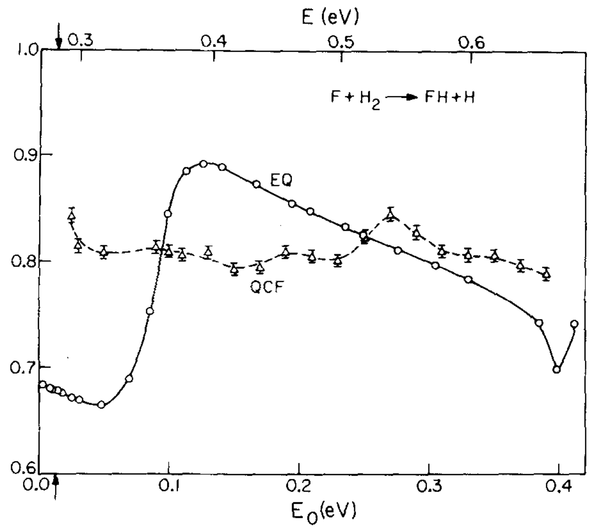

FIG. 5. Fraction (f_v) of the total reagent energy (in excess of product zero point energy) which ends up as vibrational energy in the product HF as a function of the reagent translational energy E_0 and total energy E. Solid line indicates EQ results and dashed line QCF results. Other notation analogous to Fig. 2.

well as the corresponding exact quantum ones given in Fig. 2. Out of the 100 trajectories, none yielded HF with $\nu = 0$ or 1 (i.e., $P_{01}^R = P_{00}^R = 0$ probably to within 0.01 or less). There are two important points to be noted in comparing the EQ and QCF results. First, both the exact quantum and the quasiclassical results predict roughly the same amount of vibrational excitation in the HF product on *the average*. Indeed, if we define f_v as the fraction of the total energy which ends up as vibrational energy in the product HF, then in Fig. 5 we see that f_v is roughly 0.81 and nearly independent of E_0 in the QCF results, and fluctuates between 0.66 and 0.89 with an average value of 0.79 in the EQ results. From this, we conclude that the quantum and quasiclassical dynamics agree (on the average) with respect to partitioning of product energy between translational and vibrational degrees of freedom. Second, despite this average agreement, there are very significant differences between the EQ and QCF reaction probabilities, particularly with respect to the P_{03}^R threshold and the P_{03}^R/P_{02}^R ratio. In Fig. 6 this ratio is displayed as a function of E_0 for both the EQ and QCF results. As has been pointed out previously,[19] the lack of agreement between the individual transition probabilities P_{02}^R and P_{03}^R can be partially explained as arising from the reasonable but nevertheless arbitrary way of assigning a discrete quantum number to a continuous product vibrational energy. However, the large differences in the energy dependence of the EQ and QCF $P_{0\nu}^R$ ($\nu = 2, 3$) suggests that this is probably not the whole explanation and that other significant differences exist between the classical and quantum dynamics in this system. In addition, this arbitrariness in the definition of a product quantum number is not present in the total reaction probabilities P_0^R, yet the differences in magnitude and energy dependence of the EQ and QCF results are still very significant.

It is also of interest to analyze the EQ and QCF reaction probabilities by an information theoretic approach.[13] In order to include a study of isotope effects in this analysis, we defer a discussion of this to Paper II.

In Fig. 7 are plotted the QCR and EQ reaction probabilities P_{02}^R, P_{03}^R, and P_0^R, vs E_0. The transition probability P_{02}^R is nonzero at zero reagent translational energies. This can occur because of the convention of rounding classical vibrational quantum numbers to the nearest integer.[20,33,34]

The QCR results in Fig. 7 are in much better agreement with the quantum probabilities than are the QCF results in Fig. 4. This is true not only of the total reaction probabilities P_0^R but also of the individual transition probabilities, especially P_{03}^R. The fact that the threshold behavior of the P_{03}^R transition can be described correctly by a quasiclassical method suggests that the 0.045 eV effective threshold energy in P_{03}^R(EQ) is a dynamical effect related to motion through classically accessible regions of configuration space. The fact that the reverse rather than the forward trajectory method produces the best agreement with the exact quantum results must be regarded as an empirical observation at present. It would be interesting to further analyze the quasiclassical results from the viewpoint of what regions of configuration space are being sampled by the QCR and QCF trajectories and with what velocities, and how well the current density fields derived from these trajectories agree with the corresponding exact quantum current densities.[35] The good agreement between the QCR and EQ results suggests that the QCR procedure should be applied to a three-dimensional trajectory calculation. If the differences between the one-dimensional QCR and QCF results are also found in three-dimensional calculations, this could be indicative of the presence of important quantum dynamical effects in the three-dimensional reaction.

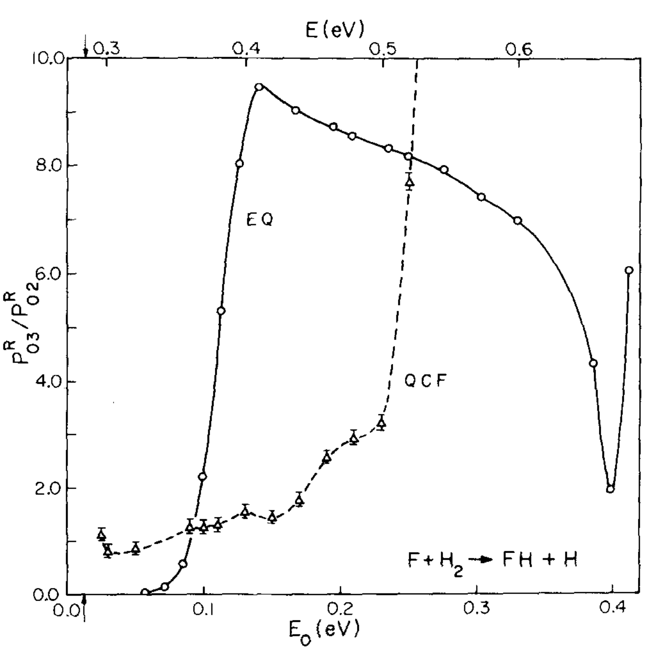

FIG. 6. Ratio of reaction probabilities P_{03}^R/P_{02}^R vs translational energy E_0 and total energy E. Solid line indicates EQ results and dashed line QCF results. Other notation analogous to Fig. 2.

Downloaded 21 Dec 2005 to 131.215.225.171. Redistribution subject to AIP license or copyright, see http://jcp.aip.org/jcp/copyright.jsp

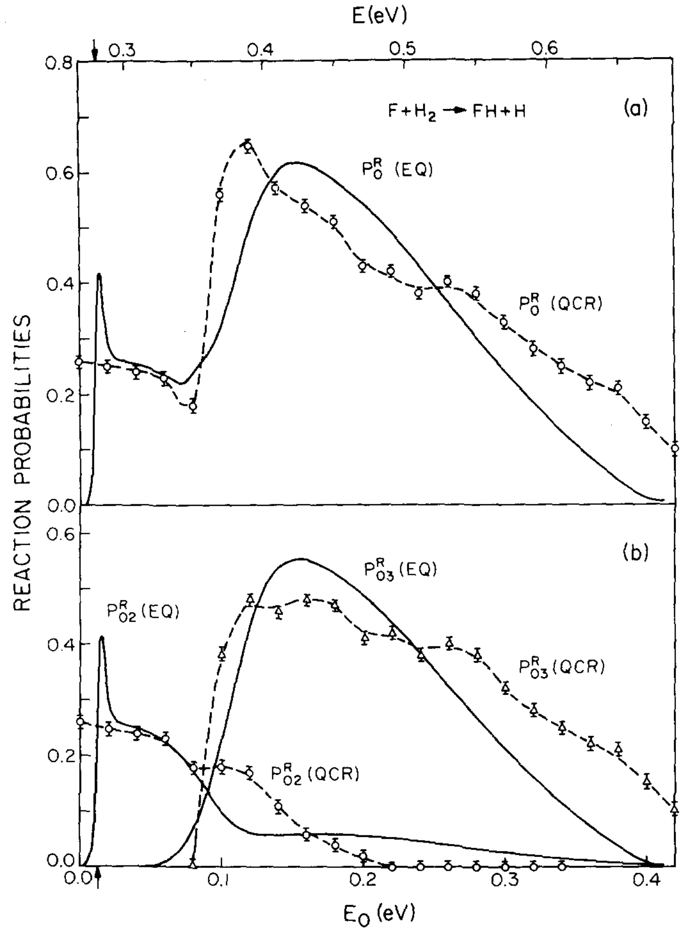

FIG. 7. Quasiclassical reverse and exact quantum reaction probabilities for $F+H_2$: (a) P_0^R, (b) P_{02}^R and P_{03}^R. Dashed line indicates QCR results with their associated statistical errors indicated by vertical bars. Solid line indicates EQ results (as in Fig. 2).

Wilkins[36] has completed a three-dimensional QCF study of the reaction $FH(\nu)+H \rightarrow H_2(\nu')+F$ (ν varying from 1 through 6). His results can be considered to be QCR calculations for the reaction $F+H_2(\nu') \rightarrow FH(\nu)+H$. He has also published QCF rate constant calculations[9a] for the latter reaction with $\nu'=0$. It would be very interesting to compare the corresponding (QCR and QCF) cross sections. Perry *et al.*[37] have recently published a three-dimensional comparison of the QCR and QCF cross sections for the endothermic $I+H_2 \rightarrow HI+I$ reaction at one total energy. They found that microscopic reversibility was approximately obeyed at this energy but made no detailed study of the energy dependence of the cross sections and did not investigate threshold effects.

C. Semiclassical reaction probabilities

1. Method

For most energies, uniform semiclassical reaction probabilities were calculated according to the procedure described in Ref. 34. However, for translational energies E_0 greater than 0.10 eV, the transition P_{02}^R was computed by a simple analytical continuation technique,[38] similar in spirit to that of Miller.[39] This was necessary in order to obtain a nonvanishing value of this transition probability, since in the above energy range, although energetically allowed, it is dynamically forbidden.[34,39] In addition, it was found that P_{03}^R was illdetermined near threshold in that a plot of final FH vibrational action number m_f vs initial H_2 vibrational phase angle (q_0) revealed "raggedness" (i.e., very rapid variation of m_f with q_0) for m_f near the value 3.[40] Raggedness was also observed over a range of energies for the $F+D_2(\nu=0) \rightarrow FD(\nu'=4)+D$ reaction by us (see following Paper II) and by Whitlock and Muckerman.[12] We managed to overcome this difficulty at several energies by doing the semiclassical analysis for the reverse reaction, i.e., $H+HF(\nu=3) \rightarrow H_2(\nu=0)+F$.[41] For this reaction, the results were considerably less ragged for m_f approximately equal to 0 than they were for the forward reaction around $m_f=3$. A more complete discussion of this procedure is given in Paper II for the $F+D_2$ reaction.

2. Results

The semiclassical reaction probabilities P_{02}^R and P_{03}^R for $F+H_2$ are presented in Fig. 8 along with the corresponding exact quantum probabilities. In the absence of considering complex-valued trajectories (in complex phase space at complex times), vanishing quasiclassical reaction probabilities implies that the corresponding semiclassical ones also vanish. Therefore, $P_{01}^R(\mathrm{USC}) = P_{00}^R(\mathrm{USC}) = 0$. From the appearance of the reaction probabilities in Fig. 8, we see that the qualitative agreement between the EQ and USC results is quite good. There are large differences between the magnitudes of the USC and EQ probabilities at certain energies, but such differences are not usually too important for the resulting collinear rate constants (see Sec. IV). Of more serious consequence for such rate constants is the small difference between the threshold energies of the P_{02}^R curves. As pointed out in Sec. III. B. 1., this threshold difference of about 0.020 eV could be partly due to an adiabatic tunneling effect, and it may be possible to improve the agreement between the EQ and USC results by using complex trajectories.[42,43]

D. Comparison of EQ, QCF, QCR, and USC reaction probabilities

In Figs. 9 and 10 we compare the exact quantum, quasiclassical forward, quasiclassical reverse, and semiclassical reaction probabilities P_{02}^R, P_{03}^R, and P_0^R for $F+H_2$ as a function of the reagent translational energy. Note that the QCR results resemble the USC ones much more than the QCF results do. Obviously, the USC threshold energy must be larger than or equal to both the QCF and QCR threshold energies. However, we cannot presently put forward an *a priori* reason that would have permitted us to predict which of the latter two energies is greater nor which of the quasiclassical reaction probabilities should be closer to the USC ones. It is also very interesting to note that the QCR results resemble the EQ ones more than the USC ones do. One should, however, be cautious not to generalize this observation. As shown in Paper II, the reverse behavior is found for the $F+D_2$ reaction.

Downloaded 21 Dec 2005 to 131.215.225.171. Redistribution subject to AIP license or copyright, see http://jcp.aip.org/jcp/copyright.jsp

IV. EQ, QCF, QCR, AND USC RATE CONSTANTS FOR $F+H_2$

The detailed $\nu \rightarrow \nu'$ rate constant for a one-dimensional bimolecular reaction such as $F+H_2(\nu) \rightarrow FH(\nu')+H$ is defined as

$$k^R_{\nu\nu'}(T) = \langle V_\nu P^R_{\nu\nu'}(V_\nu) \rangle_T = \int_0^\infty f_T(V_\nu) V_\nu P^R_{\nu\nu'}(V_\nu) dV_\nu ,$$

where V_ν is the initial relative velocity of the reagents $F+H_2(\nu)$ and $f_T(V_\nu)$ is the one-dimensional Boltzmann relative velocity distribution function. Changing the integration variable from V_ν to the initial relative reagent translational energy E_ν, this expression becomes[22]

$$k^R_{\nu\nu'}(T) = \frac{1}{(2\pi\mu_{F,HH} kT)^{1/2}} \int_0^\infty P^R_{\nu\nu'}(E_\nu) e^{-E_\nu/RT} dE_\nu .$$

Note that for one-dimensional systems, number densities are expressed in molecule/cm, so that a bimolecular rate constant has the units cm/(molecule • sec).

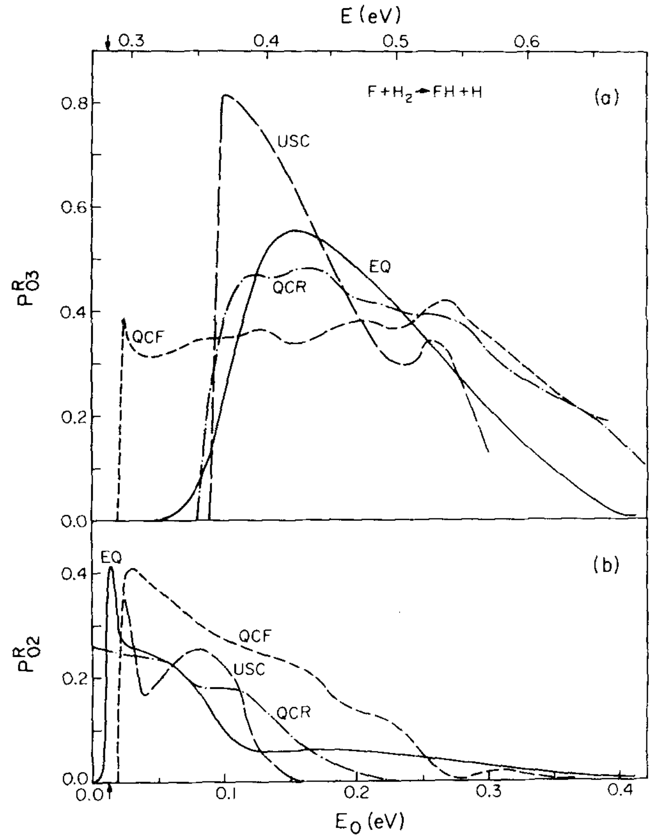

FIG. 9. EQ (solid), QCF (short dash), QCR (dash–dot), and USC (long dash) reaction probabilities P^R_{03} (a) and P^R_{02} (b) for $F+H_2$ (from Figs. 2, 4, 7, 8).

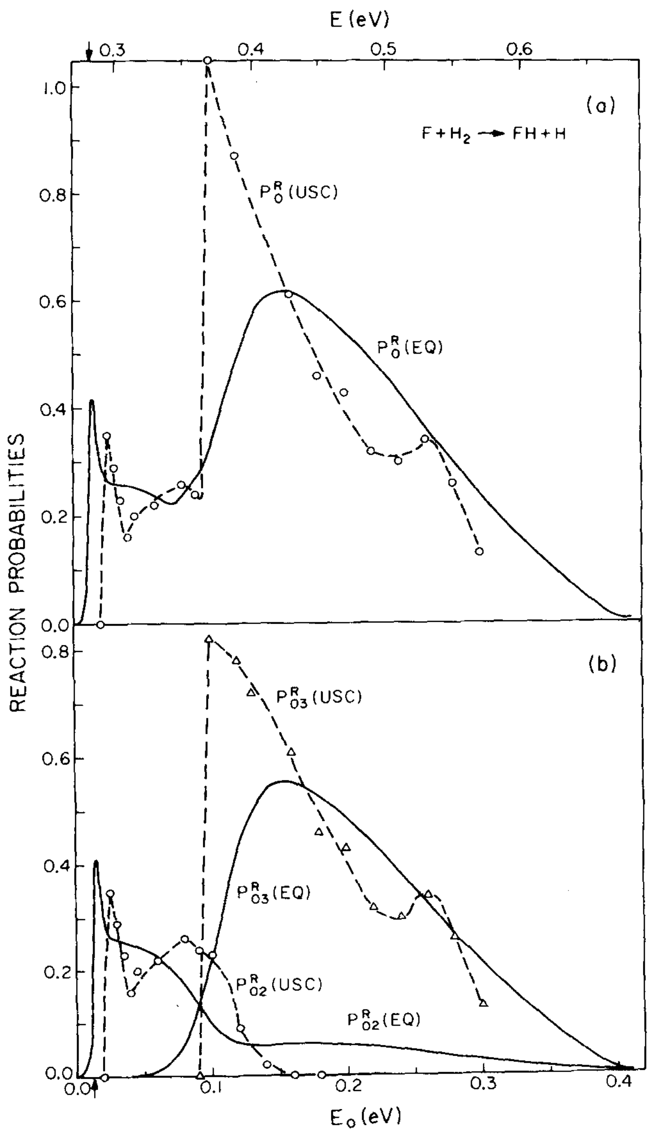

FIG. 8. Uniform semiclassical and exact quantum reaction probabilities for $F+H_2$: (a) P^R_0, (b) P^R_{02} and P^R_{03}. Dashed line indicates USC results, solid line EQ results as in Fig. 2.

Using the reaction probabilities presented in Fig. 7, we have calculated the rate constants k^R_{03} and k^R_{02} from the EQ, QCF, QCR, and USC reaction probabilities. Arrhenius plots of these rate constants are presented in Fig. 11. We see that for k^R_{03} all plots are nearly linear at high temperatures. Because of the extremely small effective threshold energies of P^R_{02}, the Arrhenius plots of k^R_{02} are only linear at low temperature (< 500 K). At high temperature, the temperature dependence of k^R_{02} approaches $T^{1/2}$, which is characteristic of a reaction with zero activation energy. Arrhenius activation energies E^{02}_a and E^{03}_a and preexponential factors A_{02} and A_{03}, which were determined by a least squares fit to the 200–400 K results and to the 900–1200 K results, are given in Table I. It is clear from Fig. 11 and Table I that k^R_{03}(QCF) has an activation energy which is significantly lower than the activation energies of k^R_{03}(EQ, QCR, or USC). This is an obvious consequence of the different effective threshold energies of the reaction probabilities (Fig. 9) and illustrates how these threshold differences can affect the detailed rate constants. As might be expected from Fig. 9, k^R_{03} (QCR) and k^R_{03}(USC) are in quite good agreement with k^R_{03}(EQ).

The relative agreement among the corresponding three k^R_{02} rate constants is much less satisfactory at low temperatures, the difference between k^R_{02}(EQ) and k^R_{02}(USC) is mainly determined by the 0.02 eV difference in the threshold energies of the P^R_{02} reaction probabilities.

Downloaded 21 Dec 2005 to 131.215.225.171. Redistribution subject to AIP license or copyright, see http://jcp.aip.org/jcp/copyright.jsp

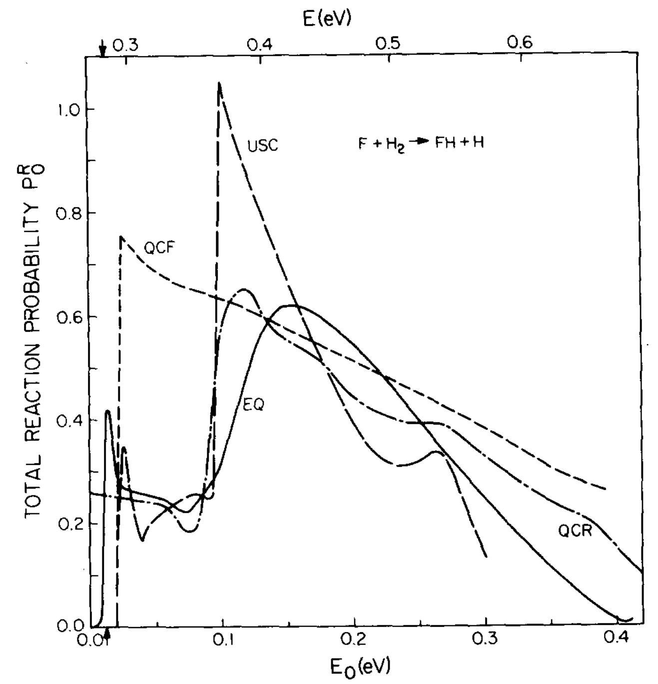

FIG. 10. EQ (solid), QCF (short dash), QCR (dash-dot), and USC (long dash) total reaction probability P_0^R for $F + H_2$ (from Figs. 2, 4, 7, 8).

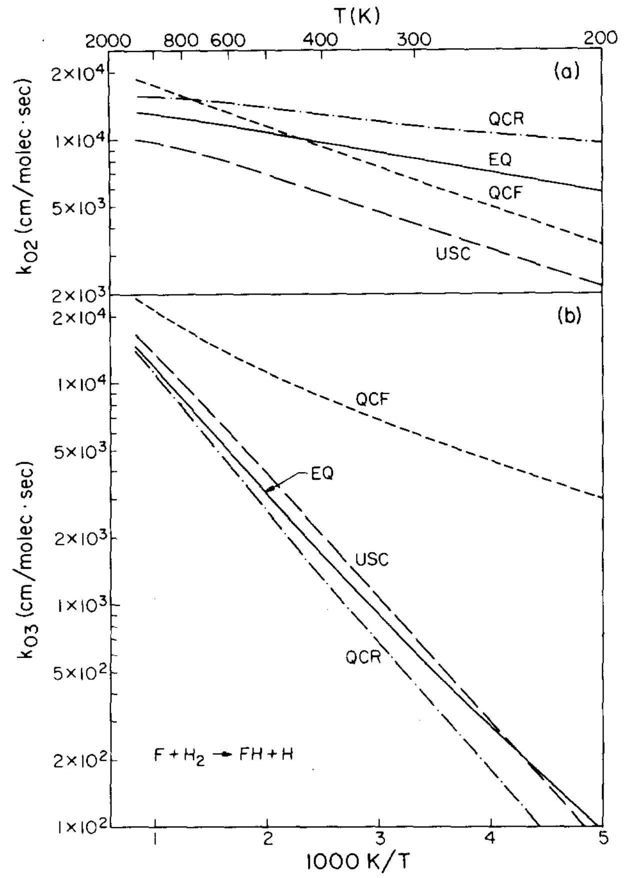

FIG. 11. Arrhenius plot of EQ (solid), QCF (short dash), QCR (dash–dot), and USC (long dash) rate constants for $F + H_2$: (a) k_{02}^R, (b) k_{03}^R.

Since P_{02}^R(QCR) has its effective threshold at zero translational energy, k_{02}^R(QCR) has a smaller activation energy than k_{02}^R(EQ), which in turn has a smaller activation energy than k_{02}^R(QCF or USC). The total rate constant k_0^R which is essentially due to the contributions of k_{03}^R and k_{02}^R does not exhibit simple Arrhenius behavior because it is the sum of two Arrhenius expressions which are of equal magnitude near $T = 1000$ K, but which have quite different activation energies. Note that the experimental activation energy (which is 1.71 kcal/mole)[44] seems to represent an average of the present EQ values of E_a^{02} and E_a^{03}.

In Fig. 12 we plot the ratio k_{03}^R/k_{02}^R as a function of temperature. The large difference between the temperature variation of the QCF ratio and that of the EQ, QCR, or USC ratios is again a consequence of the difference in the reaction probabilities in Fig. 9. It is interesting to note that the three-dimensional quasiclassical forward trajectory method yields a rate constant ratio which is nearly independent of temperature,[9a] in agreement with the one-dimensional QCF results presented here. An experimental measurement of the temperature dependence of k_{03}^R/k_{02}^R [2d] seems to agree reasonably well with the three-dimensional QCF result[9a] and consequently disagrees with our EQ result. This may indicate that the strong difference between the activation energies of k_{03}^R and k_{02}^R observed here is largely averaged out in three dimensions. On the other hand, for the $F + D_2$ reaction, the agreement between experiment and the quasiclassical results is not as consistent as it is for $F + H_2$ (to be discussed in Paper II), so it is possible that the averaging process in three dimensions does not completely destroy the important differences between the results of quantum and classical mechanics as reported in this paper.

In contrast to the k_{03}^R/k_{02}^R ratio, $k_{02}^R(\mathrm{EQ})/k_{01}^R(\mathrm{EQ})$ is nearly constant in the temperature range considered here. This agrees with the temperature variations of both the experimental[2d] and three-dimensional QCF[9a] results, although the absolute magnitudes of the ratios are quite different (~ 90 for 1-D vs ~ 3 for 3-D). We also found that $k_{01}^R(\mathrm{EQ})/k_{00}^R(\mathrm{EQ})$ is nearly independent of temperature with a value of roughly 210. Therefore k_{01}^R(EQ) and k_{00}^R(EQ) are, respectively, about 2 and 4

TABLE I. Arrhenius rate constant parameters for $F + H_2 \rightarrow FH + H$.[a]

	Temperature range (°K)	EQ	QCF	QCR	USC
E_a^{02}	200–400	0.411	0.791	0.230	0.766
E_a^{02}	200–400	2.279	0.853	2.596	2.495
A_{02}	200–400	1.620×10^4	2.424×10^4	1.669×10^4	1.486×10^4
A_{03}	200–400	2.667×10^4	2.492×10^4	3.377×10^4	4.621×10^4
E_a^{02}	900–1200	0.223	0.750	0.086	0.390
E_a^{03}	900–1200	2.628	1.444	2.869	2.368
A_{02}	900–1200	1.459×10^4	2.558×10^4	1.628×10^4	1.182×10^4
A_{03}	900–1200	4.433×10^4	4.464×10^2	4.689×10^4	4.499×10^4

[a] $k_{0i}(T) = A_{0i}\exp(-E_a^{0i}/RT)$, where E_a^{0i} is in kcal/mole and A_{0i} is in cm/(molecule · sec).

Downloaded 21 Dec 2005 to 131.215.225.171. Redistribution subject to AIP license or copyright, see http://jcp.aip.org/jcp/copyright.jsp

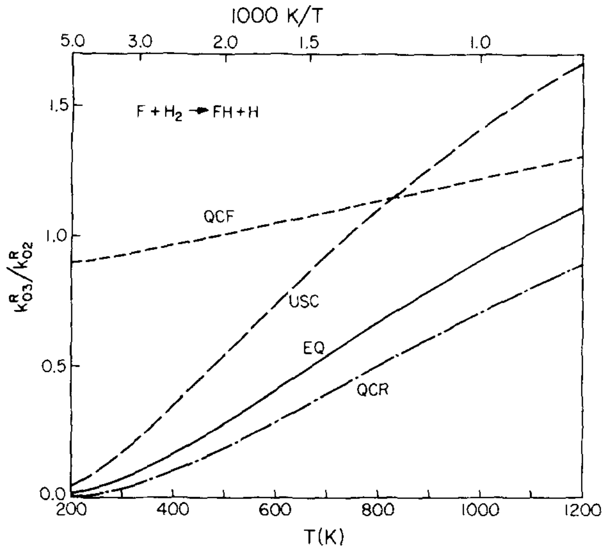

FIG. 12. Ratios of rate constants k_{03}^R/k_{02}^R for $F + H_2$ as a function of temperature. EQ (solid), QCF (short dash), QCR (dash-dot), and USC (long dash).

orders of magnitude smaller than k_{02}^R(EQ).

V. EXACT QUANTUM REACTION PROBABILITIES FOR VIBRATIONALLY EXCITED REAGENTS

In order to observe the effect of vibrational excitation of the reagent H_2 on the resulting reaction probabilities, we extended the range of our exact quantum calculations to total energies of 1.4 eV. In Fig. 13 we plot P_{02}^R, P_{03}^R, and P_{14}^R, the three largest reaction probabilities for $F + H_2$ in this energy range, as a function of energy. There are several important points to note about this figure.

First, the transition P_{14}^R has virtually zero effective threshold energy but otherwise has a similar translational energy dependence to that of P_{03}^R(which has the same $\nu' - \nu$ value as P_{14}^R). The absence of a significant threshold energy in P_{14}^R indicates that the dynamical effects responsible for the appearance of a significant effective energy threshold in P_{03}^R are no longer significant in P_{14}^R. This will lead to lower activation energies and higher rates of reaction for reagents which are initially vibrationally excited. The similarity between P_{14}^R and P_{03}^R implies that for the most significant reaction probabilities, an increase in the vibrational energy of the reagent results in a corresponding increase in the vibrational energy of the product. This agrees with experimental observations for $F + D_2$.[11]

Second, the reaction probabilities P_{03}^R and P_{14}^R have sharp peaks at $E_0 = 0.425$ eV and 0.823 eV, respectively. An analysis of the energy dependence of the scattering matrix elements corresponding to similarly shaped reaction probability curves in the $H + H_2$ collinear reaction[31,45] and in several other model reactions[46] showed that narrow peaks (or dips) in the reaction probabilities were the result of the presence of internal excitation (Feshbach) resonances. These resonances are associated with excitations of virtual states of the intermediate triatomic complex (FHH in the present case). From Fig. 13 we see that the contributions of the direct processes seem to be rather small in regions of energy where the resonance processes are important. This results in only small interference effects between direct and compound state contributions to the scattering amplitude, and the resulting reaction probabilities have nearly symmetrical peaks as a function of energy near the resonance energies. The resonance widths are about 0.01 eV, and only one nonnegligible reaction probability seems to show resonant behavior at either of the two resonance energies. There seems to be a correlation between the appearance of an internal excitation resonance and the opening of a specific vibrational state of the product (as in the resonance at 0.823 eV, which is close to the opening of the $\nu = 5$ channel in HF at 0.839 eV). This indicates a correlation of the resonance state with the reaction products rather than with the reagents or with the transition state. We shall analyze this phenomenon further in Paper II when we examine the high energy $F + D_2$ reaction probabilities.

Although the total E in Fig. 13 extends to 1.16 eV only, we have done calculations up to $E = 1.4$ eV but found all reaction probabilities in this higher energy range to be less than 0.01. This behavior seems to be related to "centrifugal" effects associated to the angle between the x_1', and z_1' axes (i.e., the skew angle between the asymptotic portions of the minimum energy path for the potential of Fig. 1) and will be further discussed in Paper II.

VI. SUMMARY

Many of the dynamical effects presented in this paper will be further examined in Paper II, to where we will relegate a more extensive summary of quantum effects in the $F + H_2$ reaction. In this paper we have seen that there are very serious differences between the results

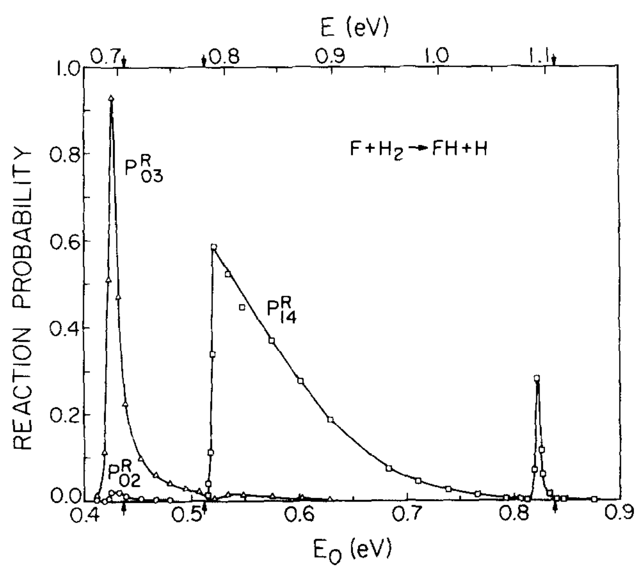

FIG. 13. Exact quantum reaction probabilities P_{02}^R, P_{03}^R, and P_{14}^R for $F + H_2$ at translational energies higher than those in Fig. 2. Arrows near $E_0 = 0.44$ eV and 0.84 eV indicate the opening of $\nu = 4$ and 5, respectively, of HF, while that at 0.51 eV indicates the energy E_0 at which $\nu = 1$ of H_2 becomes accessible.

Downloaded 21 Dec 2005 to 131.215.225.171. Redistribution subject to AIP license or copyright, see http://jcp.aip.org/jcp/copyright.jsp

of quantum and standard quasiclassical mechanics for collinear $F+H_2$, most notably in the energy dependence of the reaction probability P_{03}^R near threshold. These differences in the behavior of the reaction probabilities result in important differences in the detailed thermal rate constants. The fact that the quasiclassical forward reaction probabilities and rate constants disagree quite strongly with the exact quantum results is of great significance, since nearly all the trajectory studies done to date on this reaction have been of the quasiclassical forward type. For the present reaction, both the quasiclassical reverse and uniform semiclassical methods provide us with more accurate ways of approximating the exact quantum results. This suggests that it might be of interest to use these methods in three dimensions. Indeed, it may be possible to use the results of collinear calculations such as the ones presented here as a guideline when choosing an approximate method for doing three-dimensional calculations.

Additional exact quantum results for $F+H_2$ show that threshold effects are no longer important when the reagent H_2 is initially vibrationally excited. The dominant transitions appear to be those which channel additional vibrational energy in the reagents into additional vibrational energy in the products. Internal excitation resonances are found to play an important role in the reaction probabilities at certain translational energies. There seems to be a one-to-one correspondence between the energy at which a resonance occurs and the energy at which a related product vibrational channel opens.

ACKNOWLEDGMENT

We thank Ambassador College for the use of their computational facilities in most of the work reported here.

*Work supported in part by the United States Air Force Office of Scientific Research.

†Work performed in partial fulfullment of the requirements for the Ph.D. degree in Chemistry at the California Institute of Technology.

‡Present address: Department of Chemistry, Illinois Institute of Technology, Chicago, IL 60616.

§Contribution No. 4988.

[1](a) J. C. Polanyi and D. C. Tardy, J. Chem. Phys. **51**, 5717 (1969); (b) K. G. Anlauf, P. E. Charters, D. S. Horne, R. G. MacDonald, D. H. Maylotte, J. Polanyi, W. J. Skrlac, D. C. Tardy, and K. B. Woodall, J. Chem. Phys. **53**, 4091 (1970); (c) N. Jonathan, C. M. Melliar-Smith, and D. H. Slater, Mol. Phys. **20**, 93 (1971); (d) N. Jonathan, C. M. Melliar-Smith, D. Timlin, and D. H. Slater, Appl. Opt. **10**, 1821 (1971); (e) N. Jonathan, C. M. Melliar-Smith, S. Okuda, D. H. Slater, and D. Timlin, Mol. Phys. **22**, 561 (1971); (f) J. C. Polanyi and K. B. Woodall, J. Chem. Phys. 57, 1574 (1972); (g) H. W. Chang and D. W. Setser, J. Chem. Phys. **58**, 2298 (1973).

[2](a) K. L. Kompa and G. C. Pimentel, J. Chem. Phys. **47**, 857 (1967); (b) K. L. Kompa, J. H. Parker, and G. C. Pimentel, J. Chem. Phys. **51**, 91 (1969); (c) O. D. Krogh and G. C. Pimentel, J. Chem. Phys. **51**, 5717 (1969); (d) R. D. Coombe and G. C. Pimentel, J. Chem. Phys. **59**, 251 (1973); (e) W. H. Green and M. C. Lin, J. Chem. Phys. **54**, 3222 (1971); (f) M. J. Berry, J. Chem. Phys. **59**, 6229 (2973).

[3](a) T. P. Schaefer, P. E. Siska, J. M. Parson, F. P. Tully, Y. C. Wong, and Y. T. Lee, J. Chem. Phys. **53**, 3385 (1970); (b) Y. T. Lee (VII ICPEAC), *The Physics of Electronic and Atomic Collisions*, edited by T. R. Govers and F. J. de Heer (North-Holland, Amsterdam, 1971), p. 357.

[4]See compilations by N. Cohen, Report No. TR-0073(3430)-9, The Aerospace Corporation, El Segundo, CA, 1972 and Report No. TR-0074(4530)-9, The Aerospace Corporation, El Segundo, CA, 1974.

[5]A. Persky, J. Chem. Phys. **59**, 5578 (1973).

[6](a) D. J. Spencer, T. A. Jacobs, H. Mirels, and R. W. F. Gross, Int. J. Chem. Kinet. **1**, 493 (1969); (b) T. F. Deutsch, Appl. Phys. Lett. **10**, 234 (1967); (c) S. N. Suchard, R. L. Kerber, G. Emanuel, and J. S. Whittier, J. Chem. Phys. **57**, 5065 (1972) and references therein.

[7](a) J. T. Muckerman, J. Chem. Phys. **54**, 1155 (1971); (b) 56, 2997 (1972).

[8](a) R. L. Jaffe and J. B. Anderson, J. Chem. Phys. **54**, 2224 (1971); (b) 56, 682 (1972); (c) R. L. Jaffe, J. M. Henry, and J. B. Anderson, J. Chem. Phys. **59**, 1128 (1973).

[9](a) R. L. Wilkins, J. Chem. Phys. **56**, 912 (1972); (b) R. L. Wilkins, J. Phys. Chem. **77**, 3081 (1973).

[10]N. C. Blais and D. G. Truhlar, J. Chem. Phys. **58**, 1090 (1973).

[11]A. Ding, L. Kirsch, D. Perry, J. Polanyi, and J. Schreiber, Discuss. Faraday Soc. **55**, 252 (1973).

[12]P. A. Whitlock and J. T. Muckerman, J. Chem. Phys. **61**, 4618 (1975).

[13](a) A. Ben-Shaul, R. D. Levine, and R. B. Bernstein, Chem. Phys. Lett. **15**, 160 (1972); (b) A. Ben-Shaul, R. D. Levine, and R. B. Bernstein, J. Chem. Phys. **57**, 5427 (1972); (c) A. Ben-Shaul, G. L. Hofacker, and K. L. Kompa, J. Chem. Phys. **59**, 4664 (1973).

[14]G. L. Hofacker and R. D. Levine, Chem. Phys. Lett. **15**, 165 (1972), also unpublished results.

[15](a) C. F. Bender, S. V. O'Neil, P. K. Pearson, and H. F. Schaefer, III, Science **176**, 1412 (1972); (b) C. F. Bender, P. K. Pearson, S. V. O'Neil, and H. F. Schaefer, III, J. Chem. Phys. **56**, 4626 (1972).

[16]D. G. Truhlar, J. Chem. Phys. **56**, 3189 (1972).

[17]J. T. Muckerman and M. D. Newton, J. Chem. Phys. **56**, 3191 (1972).

[18]J. C. Tully, J. Chem. Phys. **60**, 3042 (1974).

[19]G. C. Schatz, J. M. Bowman, and A. Kuppermann, J. Chem. Phys. **58**, 4023 (1973).

[20]J. M. Bowman, G. C. Schatz, and A. Kuppermann, Chem. Phys. Lett. **24**, 378 (1974).

[21](a) P. J. Kuntz, E. M. Nemeth, J. C. Polanyi, S. D. Rosner, and C. E. Young, J. Chem. Phys. **44**, 1168 (1966); (b) J. C. Polanyi and W. H. Wong, J. Chem. Phys. **51**, 1439 (1969).

[22]D. Truhlar and A. Kuppermann, J. Chem. Phys. **56**, 2232 (1972).

[23](a) R. Saxon and J. Light, J. Chem. Phys. **56**, 3874 (1972); (b) 56, 3885 (1972); (c) G. Wolken and M. Karplus, J. Chem. Phys. **60**, 351 (1974); (d) A. B. Elkowitz and R. E. Wyatt, J. Chem. Phys. **62**, 2504 (1975).

[24](a) A. Kuppermann, G. C. Schatz, and M. Baer, J. Chem. Phys. **61**, 4362 (1974); (b) A. Kuppermann and G. C. Schatz, J. Chem. Phys. **62**, 2502 (1975).

[25]J. T. Muckerman (private communication).

[26]L. M. Delves, Nucl. Phys. **20**, 275 (1960).

[27]G. Glasstone, K. Laidler, and H. Eyring, *Theory of Reaction Rates* (McGraw Hill, New York, 1941), p. 101; M. Karplus and K. Tang, J. Chem. Phys. **50**, 1119 (1970).

[28](a) A. Kuppermann, *Potential Energy Surfaces in Chemistry*, edited by W. A. Lester (University of California at Santa Cruz, 1970), pp. 121–129; (b) Abstracts of papers, (VII ICPEAC), *Electronic and Atomic Collisions*, edited by L. Branscomb (North-Holland, Amsterdam, 1971), p. 3.

[29]D. G. Truhlar, J. Comput. Phys. **10**, 123 (1972).

[30]The reaction probabilities were found to be independent of the location of the endpoints of the integrations in each arrange-

Downloaded 21 Dec 2005 to 131.215.225.171. Redistribution subject to AIP license or copyright, see http://jcp.aip.org/jcp/copyright.jsp

ment channel before the potential had completely reached its asymptotic value. However, the translational energies computed at the points of termination of the integrations were slightly smaller than their correct asymptotic values. The results reported here have been corrected by the difference (less than 0.0002 eV).

[31]G. C. Schatz and A. Kuppermann, J. Chem. Phys. 59, 964 (1973).

[32]G. C. Schatz and A. Kuppermann (to be published).

[33]J. M. Bowman and Aron Kuppermann, Chem. Phys. Lett. 12, 1 (1972).

[34]J. M. Bowman and Aron Kuppermann, J. Chem. Phys. 59, 6524 (1973).

[35]A. Kuppermann, J. T. Adams, and D. G. Truhlar, *Abstracts of Papers, Eighth International Conference on the Physics of Electronic and Atomic Collisions*, edited by B. C. Cobic and M. V. Kurepa (Institute of Physics, Belgrade, 1973), p. 149.

[36]R. L. Wilkins, J. Chem. Phys. 58, 3038 (1973).

[37]D. S. Perry, J. C. Polanyi, and C. W. Wilson, Chem. Phys. Lett. 24, 484 (1974).

[38]J. M. Bowman, Ph.D. thesis, California Institute of Technology, 1974.

[39]W. H. Miller, Chem. Phys. Lett. 4, 431 (1970); J. Chem. Phys. 53, 3578 (1970).

[40]C. C. Rankin and W. H. Miller, J. Chem. Phys. 55, 3150 (1971).

[41]This procedure is obviously valid if the function $m_f(q_0)$ is "smooth" (i.e., nonragged) for both the forward and reverse trajectories, since under these conditions, semiclassical reaction probabilities (contrarily to quasiclassical ones) rigorously obey microscopic reversibility.[34] As a result, when one of these $m_f(q_0)$ is smooth and the other not, it is reasonable to associate the semiclassical reaction probability of both the forward and reverse reactions to the smooth $m_f(q_0)$.

[42]W. H. Miller and T. F. George, J. Chem. Phys. 56, 5668 (1972); J. Chem. Phys. 57, 2458 (1972).

[43]For the $H+H_2$ reaction, the complex trajectory method yields reaction probabilities differing by less than 30% from the exact quantum results for energies less than the barrier (Ref. 32).

[44]G. C. Fettis, J. H. Knox, and A. F. Trotman-Dickenson, J. Chem. Soc. 1960, 1064.

[45]R. D. Levine and S. F. Wu, Chem. Phys. Lett. 11, 557 (1971).

[46]S. F. Wu, B. R. Johnson, and R. D. Levine, Mol. Phys. 25, 839 (1973).

Downloaded 21 Dec 2005 to 131.215.225.171. Redistribution subject to AIP license or copyright, see http://jcp.aip.org/jcp/copyright.jsp